Measurements of anomalous elastic scattering of 59.54-keV photons

C. Baraldi, E. Casnati, A. Tartari, M. Andreis, and B. Singh*
Dipartimento di Fisica dell'Università, I-44100 Ferrara, Italy and Istituto Nazionale di Fisica Nucleare, Sezione di Ferrara, I-44100, Ferrara, Italy
(Received 16 May 1996)

Coherent scattering cross sections of 59.54-keV photons on target foils of ^{64}Gd, ^{66}Dy, ^{68}Er, ^{70}Yb, ^{72}Hf, and ^{73}Ta at 60°, 90°, and 120° have been measured to provide information on the region of *K* anomalous elastic scattering. The results are compared with the values calculated by the second perturbative order *S* matrix and by two procedures based on the form-factor approximation corrected by the anomalous scattering factors. Agreement of the *S* matrix values is very satisfactory, on the whole, and that of the values given by the form-factor approximations is fairly good. [S1050-2947(96)08311-4]

PACS number(s): 32.80.Cy

INTRODUCTION

The opportunity of concise, easy to read tabulations of elastic-coherent-scattering amplitudes and hence of the relevant atomic cross sections, both differential and total, has been stressed more than once in recent years [1–3]. Completeness and accuracy are also important prerequisites. In fact, the QED approach by *S* matrix, even if restricted to the second perturbative order (SM) by the independent-particle approximation (IP) as proposed by Kissel, Pratt, and Roy [4] and by Kissel and Pratt [5], cannot be used systematically because the computing time grows prohibitively with the number and complexity of the atomic electron shells, and complete tabulations would be excessively cumbersome. On the other hand, the values given by the various form-factor approximations are easy to tabulate, as they are functions of the momentum transfer alone, but they also show deviations from the SM calculated or experimentally measured values which, though acceptable for some applications, give results unacceptably far from the correct ones in other cases.

The form-factor approximation does not, in fact, include the dispersive effects at energies close to the photoeffect thresholds and, therefore, the amplitudes calculated by such approximation are inaccurate near those thresholds, and also at incident-photon energies lower than the *K* threshold [1,4]. The atomic form factor is the Fourier transform of the atomic charge distribution and can be evaluated by different wave functions. At present, extensive tabulations of the form factor calculated with either nonrelativistic [6] or relativistic (RF) [7] wave functions are available. The modified relativistic form factor (MF) proposed by Franz [8] uses a relativistic wave function, and also considers the corrections due to electron bindings. Therefore, its atomic value is the sum of those pertinent to each shell, and it gives more correct amplitudes at high atomic number and the right forward scattering high-energy relativistic limit [9,10]. A tabulation of MF's for the whole atom and the atom without the *K* shell, which covers all the elements of the periodic table, was prepared by Schaupp *et al.* [11].

In order to reduce the deviations of the elastic-coherent-scattering amplitudes calculated by the atomic form-factor approximations in the region of photoeffect thresholds from the experimental values, Kronig [12] and Kramers [13] introduced the anomalous scattering factors evaluated by means of the dispersion relations, which relate the real and imaginary parts of the forward-scattering amplitudes, and the optical theorem, which relates the imaginary part of the forward-scattering amplitude to the photoabsorption cross section. As further conditions are unavailable, these factors are supposed to be independent from the scattering angle and combined with the form factor to give the elastic-coherent-scattering amplitudes. Different tabulations of the anomalous scattering factors, which mainly differ in the approximation chosen for the high-energy limit, have been obtained by many authors [14–20]. Chantler [21] employed the high-energy relativistic limit obtained by including the quadrupole and retardation effects in the perturbation theory, and prepared a tabulation of the anomalous scattering factors which, thanks to a careful revision of the relevant expressions, gives qualitative and quantitative improvements, especially at incident-photon energies above 30–60 keV and near the photoeffect thresholds. Kissel *et al.* [3] proposed the use of the relativistic modified form factor, which gives essentially the correct high-energy limit, together with the appropriate anomalous scattering factors and compared the results given by that approach for C and Pb with those obtained by the SM method within the IP.

A procedure for accurate evaluation of the coherent-elastic-scattering amplitudes, the values of which unfortunately cannot be synthetically tabulated, was elaborated by Kissel, Pratt, and Roy [4] and by Kissel and Pratt [5]. The code of these authors combines the numerical evaluations given by the SM approach within the IP for the innermost atomic shells with those obtained from the MF approximation and the scale factor provided by the optical theorem, respectively, for the real and imaginary parts of the amplitudes due to the remaining shells. The independent-particle approximation assumes that the electrons move freely in the nuclear field, and therefore neglects the electron correlation effects. Such effects have no evident consequences in many situations, but can give rise to appreciable deviations at low-incident photon energies, or in proximity to the photoeffect

*Permanent address: Physics Department, Punjabi University, Patiala, India.

TABLE I. Properties of the scattering foils. Z, atomic number; E_K, photoeffect threshold energy [37]; E_i/E_K, ratio between photon and K photoeffect threshold energies; P, purity; L, mass thickness; s_L, standard deviation of the mass thickness on the whole irradiated area; $f_{\pi/4}$, effective saturation at $\pi/4$ reflection angle.

Target element	Z	E_K (keV)	E_i/E_K	P (%)	L (mg/cm^2)	s_L (mg/cm^2)	$f_{\pi/4}$
Be	4	0.1117		99.9	103.30	0.26	0.0401
Gd	64	50.239	1.185	99.9	82.82	0.10	0.939
Dy	66	53.788	1.107	99.9	112.58	0.11	0.984
Er	68	57.486	1.036	99.9	96.42	0.40	0.977
Yb	70	61.332	0.971	99.9	67.26	0.17	0.429
Hf	72	65.351	0.911	97.0	331.84	0.48	0.950
Ta	73	67.413	0.883	99.9	450.06	0.53	0.986

threshold [3]. Therefore, controls of the reliability of this code near the absorption threshold of the innermost shells, and particularly of the K shell, can be really interesting.

Kane *et al.* [22] brought out an extensive comparison, not specifically concerned with K anomalous elastic scattering, between the atomic elastic coherent cross section given by Kissel and Pratt's code and the experimental values available at the time for various elements and photon energies. Experimental measurements of atomic coherent differential scattering cross sections with and without a specific reference to the K energy region, but with data falling in that region, have been carried out by many authors (e.g., [2,23–32]).

The present paper gives the results of measurements of the atomic coherent cross section at 60°, 90°, and 120° of 59.54-keV photons impinging on six target elements with $64 \leqslant Z \leqslant 73$ and, therefore, with threshold energies close to that of the incident photons. The results are compared with the values obtained by means of the SM code of Kissel, Pratt, and Roy [4] by Kissel [33] (SMK), with those based on MF and anomalous scattering factors [3] calculated by Kissel [34] (MFK), and with those calculated from RF and Chantler's anomalous scattering factors [21] (RFC). The measurements were carried out by the high-precision goniometric irradiation bench already used for measurements of

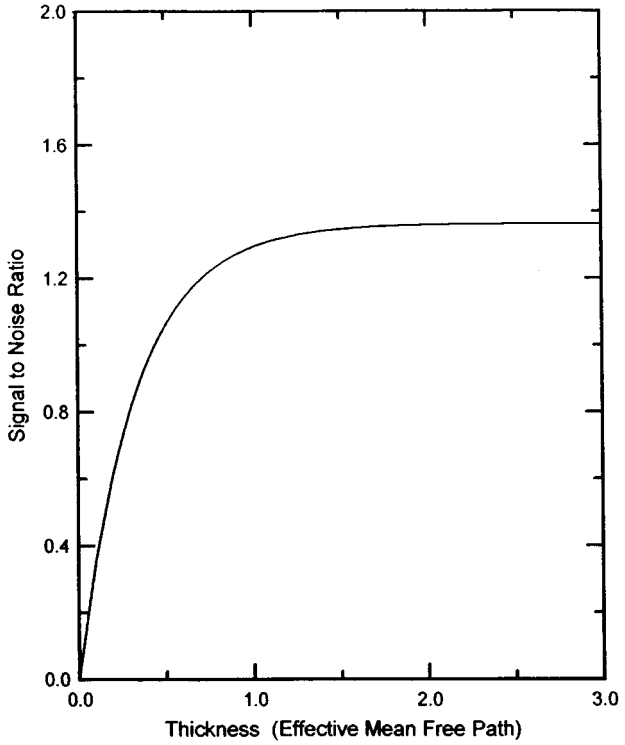

FIG. 1. Signal-to-noise ratio of the ^{68}Er scattering foil as function of thickness.

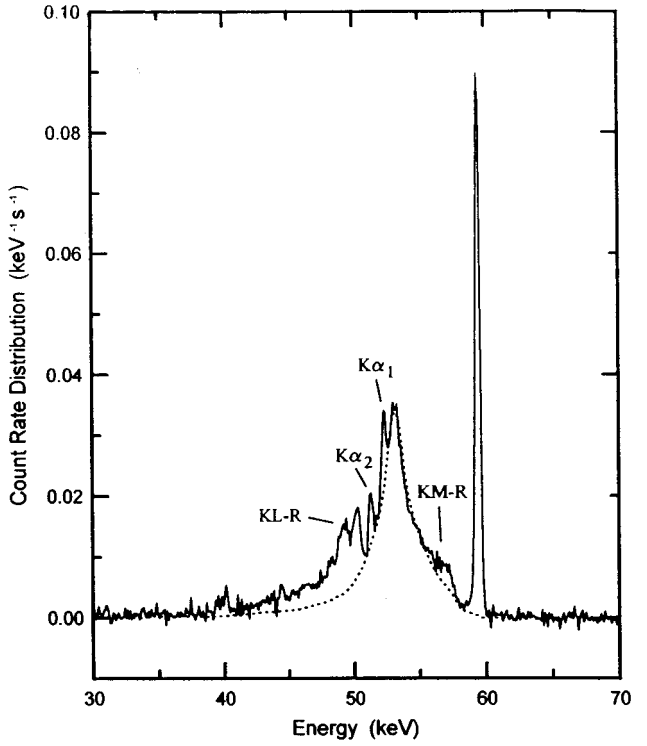

FIG. 2. ^{70}Yb spectral distribution of 59.54-keV photons scattered at 90°. Continuous line, experimental data corrected for external background only; dotted line, Compton scattering spectrum calculated from Compton profile. $K\alpha_1$ and $K\alpha_2$ are photoelectric K peaks, and KL-R and KM-R resonance Raman distributions.

TABLE II. Coherent-scattering differential cross section of 59.54-keV photons. Z, atomic number; ϑ, scattering angle; σ'_{Ex}, experimental values; s, standard deviation of experimental values; s_r, relative standard deviation of experimental values; SMK, values based on S matrix [33]; MFK, values calculated by the modified form factor procedure [34]; RFC, values obtained from the relativistic form factor procedure [21].

Target element	Z	ϑ	σ'_{Ex} (b/sr)	s (b/sr)	s_r (%)	SMK (b/sr)	MFK (b/sr)	RFC (b/sr)
Gd	64	60°	3.671	0.055	1.5	3.70	3.826	3.554
Dy	66		3.841	0.077	2.0	3.78	3.903	3.653
Er	68		3.494	0.070	2.0	3.42	3.534	3.364
Yb	70		2.927	0.035	1.2	3.02	3.203	2.985
Hf	72		4.003	0.056	1.4	4.14	4.293	4.012
Ta	73		4.289	0.060	1.4	4.51	4.687	4.371
Gd	64	90°	1.201	0.018	1.5	1.16	1.222	1.103
Dy	66		1.181	0.024	2.0	1.13	1.190	1.081
Er	68		0.980	0.020	2.0	0.936	0.9952	0.924
Yb	70		0.542	0.014	2.5	0.557	0.6204	0.538
Hf	72		0.923	0.012	1.3	0.970	1.027	0.893
Ta	73		1.076	0.014	1.3	1.11	1.181	1.026
Gd	64	120°	0.999	0.016	1.6	1.02	1.087	0.970
Dy	66		0.993	0.020	2.0	0.964	1.036	0.931
Er	68		0.809	0.016	2.0	0.778	0.8447	0.782
Yb	70		0.282	0.013	4.7	0.292	0.3397	0.265
Hf	72		0.5693	0.0080	1.4	0.594	0.6397	0.523
Ta	73		0.6689	0.0094	1.4	0.689	0.7475	0.612

the same quantity on elements with Z far from the anomalous scattering region.

MEASUREMENT METHODOLOGY

The geometrical arrangements and experimental methodology have been described in detail elsewhere by Casnati, Baraldi, and Tartari [35,36], and only those aspects that are essential to the interpretation of the present results will be recalled here. Both the 18.5-GBq ^{241}Am source and the 200-mm^2 hyperpure Ge detector, 10 mm thick, were provided with multivane collimators that restricted the solid angle of primary beam emission, that of detector acceptance, and the target surface seen by the detector. This surface had such dimensions that ensured it was illuminated by the whole source. The geometry was specular, i.e., the angles formed by the axes of the incident and measured beams with the normal to the surface of the target foil were equal. The nominal distances between source and target and between target and detector were approximately equal to one another, and the acceptance angle of the detector was rather small. The experimental arrangement gave rise to an angular response function with a full width at half maximum of about 4° in the scattering plane defined by the incidence and scattering axes.

The measurements of the coherent differential cross section σ'_{Ex} have been normalized to those of the ^{4}Be incoherent differential cross section $\sigma'_{\mathrm{KN}}S_{\mathrm{Be}}$, where σ'_{KN} is the Klein-Nishina electron cross section, and S_{Be} the ^{4}Be scattering function that equals four to within a few parts per thousand. The expression giving the differential atomic coherent scattering cross section is then

$$\sigma'_{\mathrm{Ex}}=\sigma'_{\mathrm{KN}}S_{\mathrm{Be}}\,\frac{\alpha_{\mathrm{Be}}\beta_{\mathrm{Be}}M_x}{\alpha_x\beta_xM_{\mathrm{Be}}}\,\frac{N_{\mathrm{Ex}}}{N_{I\mathrm{Be}}}.$$

The factor α has the dimension of thickness and corrects the target autoattenuation, while β accounts for the physical efficiency of the detector and the air attenuation. Their expressions are

$$\alpha=\rho\,\frac{1-\exp[-(\mu_i+\mu_e)L/\cos\gamma]}{\mu_i+\mu_e},$$

$$\beta=\epsilon\,\exp(-\mu_aL_a),$$

where ρ and L are the density and thickness of the foil target, μ_i and μ_e its attenuation coefficients for incident and emerging radiation, and γ the reflection angle. μ_a and L_a are the attenuation coefficient and thickness of the air lying between target and detector, and ϵ is the detector physical efficiency. N_{Ex} and $N_{I\mathrm{Be}}$ are, respectively, the coherent counts measured with the target element of interest and the incoherent ones given by the ^{4}Be target, both normalized to the unit of time. The values of all the parameters were randomized whenever possible; e.g., the positioning of any one of the measurements carried out more than once at each of the three angles was individually repeated each time.

The properties of the examined solid targets are given in Table I, which also includes the saturation factor for the $\pi/2$ scattering angle, corresponding to the $\pi/4$ reflection angle, $f_{\pi/4}=1-\exp[-(\mu_i+\mu_e)L\sqrt{2}]$. Most of the targets, with the sole exception of ^{4}Be and ^{70}Yb, have thicknesses close to saturation, i.e., of the order of three mean-free paths or a little more. This choice assures the greatest signal-to-noise ratio as shown by Fig. 1, where such a ratio for ^{68}Er is represented as a function of the target thickness measured in effective mean-free-path $1/\overline{\mu}=2/(\mu_i+\mu_e)$ units. The background counting in the signal region is the sum of the components arising from electronics and environmental radiation

and of that caused by the target multiple scattering, really restricted to the second order. The first component is obtained by the analysis of the countings carried out without the radiation beam and of those with the radiation beam but without the target, in order to also evaluate the amount of the incoherent scattering of air that could affect the reference measurements made with the ^{4}Be foil. The second component is calculated by the expression given by Casnati *et al.* [38] This expression was evaluated by the RFC cross sections for which a maximum uncertainty of 10% was assumed; this approach was justified by the smallness of the double-scattering contribution, which only exceptionally reaches 10% of that of the single scattering. It is to be pointed out that, for thickness $L/\cos\gamma$ close to zero or to saturation, the parameter α becomes, respectively,

$$\alpha \approx \frac{\rho L}{\cos\gamma}, \quad \alpha \approx \frac{\rho}{\mu_i + \mu_e}.$$

Therefore, the α value mainly depends on the oblique thickness of the target when this is very thin, and on the attenuation coefficients of the target material when it is rather thick. In order to assure good accuracy of the attenuation coefficient, the average values of the tabulations of Veigele [39], Storm and Israel [40], Plechaty, Cullen, and Howerton, [41] and of that of Scofield [42] combined with that of Hubbell *et al.* [6] were used. Moreover, direct measurements of the attenuation coefficients of 59.54-keV photons in the elements of interest were carried out and the results obtained agreed very well with the used averages within the experimental uncertainties.

The corrections for the presence of external and internal background, for the recombination charge loss, for the K escape peak, and for the asymmetry of the instrumental peak were applied to the area evaluation of both calibration and coherent signals. Moreover, the coherent signals were corrected for the Compton scattering radiation with its discontinuities caused by the electron bindings, for the possible Raman resonances, and for the K peaks stimulated by the components of high energy present in the incident beam. Figure 2 shows the ^{70}Yb experimental spectrum corrected only for the external background contribution. In the same figure is drawn the incoherently scattered spectrum as given by the distribution calculated from the Compton profiles tabulated by Biggs, Mendelsohn, and Mann [43] convoluted with the spectrometer response function and corrected for target autoattenuation and air and detector attenuations. This spectrum helps in correcting the contribution of the incoherent scattered radiation. The $K\alpha_1$ and $K\alpha_2$ peaks produced by the incident high-energy component emitted by the ^{241}Am source are evident, as are the KL and KM resonant Raman distributions. Both the characteristic $K\beta$ and Raman KN signals fall within the energy interval of the coherent peak and, therefore, must be subtracted from the experimental spectrum. The $K\beta$ contribution has been evaluated by applying to the experimental spectrum the procedure described by Casnati *et al.* [44], whereas the KN has been neglected as its amount is negligible with respect to the coherent signal [45].

EXPERIMENTAL RESULTS AND DISCUSSION

The experimental results obtained by the described procedure are collected in Table II, together with their uncertainties expressed in terms of both absolute and relative standard deviations. In the same table are given the relevant SMK values. For completeness, the MFK and RFC values are also included. The necessary interpolations were always performed by Lagrangian polynomials. The effect of solid-state environment on the measurements of coherent-scattering cross section has to be considered negligible in the explored 2.40–4.16 momentum transfer interval and, therefore, the results can be compared with the calculations performed on free atoms.

In these comparisons special care has been devoted to checking the consistency of SMK values with the experimental ones because, as pointed out by Kissel *et al.* [3]; also this code, though detailed and accurate, could give rise to deviations of some percent in proximity of the photoeffect thresholds. Figure 3 shows the dependence on Z of SMK values for 59.54-keV photons scattered at 90° and the relevant values of the present experiment.

A preliminary analysis proves that, in most cases, the deviations of the SMK values from the experimental ones are not consistent with the uncertainties of the latter, and the χ^2 test confirms the lack of agreement between experimental and calculated data in the region of the K photoeffect threshold at the angles and photon energy considered. A greater disagreement is shown from the results of MFK and RFC calculations. A careful control of the parameter values and of

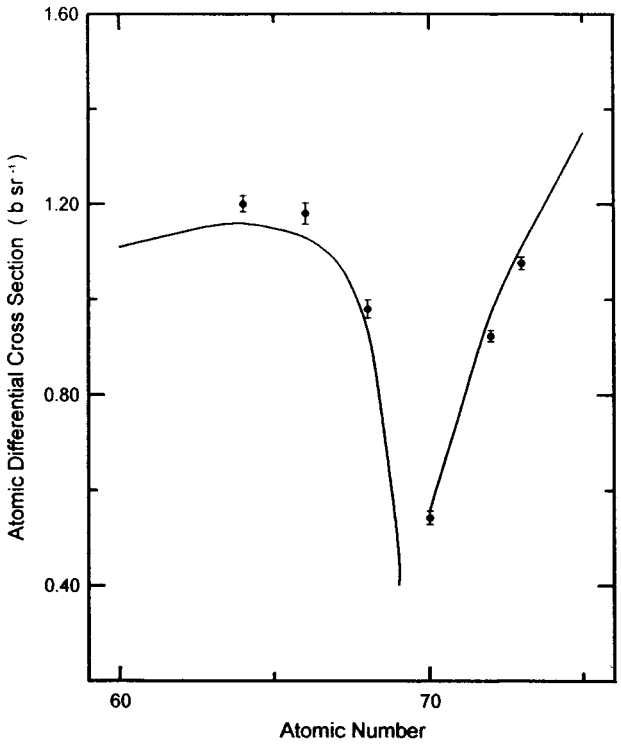

FIG. 3. Atomic elastic differential cross section vs atomic number. Continuous line, values of Kissel [34]; points, experimental values. Bars represent standard deviations.

TABLE III. Calculated coherent differential cross section of 59.54-keV photons normalized to experimental values. Z, atomic number; ϑ, scattering angle; SMK_N, normalized SMK values; MFK_N, normalized MFK values; RFC_N, normalized RFC values.

Target element	Z	ϑ	SMK_N	MFK_N	RFC_N
Gd	64	60°	1.008	1.042	0.968
Dy	66		0.984	1.016	0.951
Er	68		0.979	1.011	0.963
Yb	70		1.032	1.094	1.020
Hf	72		1.034	1.072	1.002
Ta	73		1.052	1.093	1.019
Gd	64	90°	0.966	1.017	0.918
Dy	66		0.957	1.008	0.915
Er	68		0.955	1.016	0.943
Yb	70		1.028	1.145	0.993
Hf	72		1.051	1.113	0.968
Ta	73		1.032	1.098	0.954
Gd	64	120°	1.021	1.088	0.971
Dy	66		0.971	1.043	0.938
Er	68		0.962	1.044	0.967
Yb	70		1.035	1.205	0.940
Hf	72		1.043	1.124	0.919
Ta	73		1.030	1.118	0.915

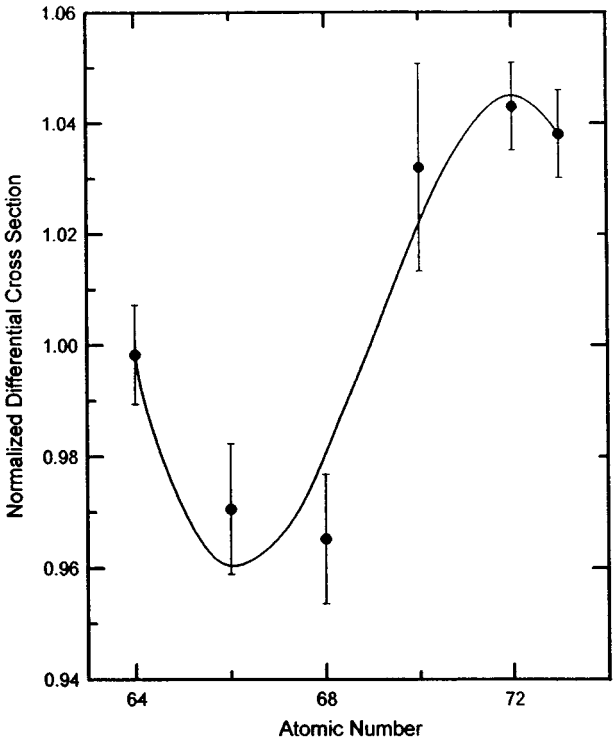

FIG. 4. S matrix calculated atomic differential cross sections normalized to experimental data vs atomic numbers. Points and bars, values and standard deviations; continuous line, least-square interpolation by a third-degree polynomial.

the procedure used in processing the experimental data and evaluating the uncertainties was, therefore, carried out, but no mistakes were found.

In order to aid understanding of the nature of these deviations and to detect some possible regular behavior, the normalized SMK_N, MFK_N, and RFC_N values were calculated as the ratios of SMK, MFK, and RFC to the relevant experimental values. The results are collected in Table III. Their uncertainties, which are due to the experimental dividend, are practically equal to the relative uncertainties of the experimental data. The SMK_N have a grand mean of 1.008, i.e., very close to the unity, while those of MFK_N and RFC_N are 1.075 and 0.959, respectively. Moreover, the angular variabilities of the SMK_N values are well consistent with the experimental uncertainties, whereas those of MFK_N and RFC_N are greater than what could be justified by the experimental uncertainties.

Regular behavior seems instead to be followed inside each elemental series, i.e., the series of the normalized values at each angle for the examined elements with Z increasing from 64 to 73. In fact, in each of the nine series except one the first three values are lower and the last three higher than the mean of the individual series. To examine the trends of these regular deviations with Z, SMK_N values were employed, because their angular independence makes it possible to improve the significance of the analysis by operating on angular averages. These angular averages are presented as points with their uncertainty bars in Fig. 4. The continuous line in the same figure shows the least-square third-degree polynomial that fits those values rather satisfactorily and confirms a regular excursion of SMK_N ratios of about $\pm 4\%$. A behavior of this kind can be ascribed to either the used K threshold values [3] or the gradient with Z of the calculated elastic-scattering cross section, in one or in both of its branches near the K thresholds. Within the limits of the present experiment, differences of the order of some tenth percent or up to ten percent in the first and second case, respectively, could explain the observed trend; of course, both the effects can act together.

It is to be observed that at least for Ta many authors [24,26,29,30,46] have measured the elastic differential cross section of 59.54-keV photons scattered at various angles, and it is worthwhile to note that the mean, 1.042 ± 0.018, of the ten SMK_N ratios obtained from the data falling within 15% of the SMK values agrees very well with the mean of the three values given by the present experiment, 1.038 ± 0.008. Also the SMK_N ratio calculated by the experimental result of Varier and Unnikrishnan [29] on ^{70}Yb, the only one value on this element falling within the $\mp 15\%$ interval around the relevant SMK datum, agrees very well with the present one: 0.994 ± 0.074 and 1.032 ± 0.018, respectively. The agreement between the SMK_N averages evaluated by either the experimental data given at four scattering angles by Nandi *et al.* [27] for ^{68}Er and those of the present work is less satisfactory; in fact, the respective values are 1.034 ± 0.026 and 0.965 ± 0.012. This difference, to be ascribed mainly to the deviation of the Nandi *et al.* value at 60° from the SMK one, could arise from the difficulty of angle estimates in an angular region where the cross section changes very rapidly, as the authors also remark. Comparison of the present SMK_N values with those which can be obtained from the experiments carried out by other authors on ^{64}Gd and ^{66}Dy should have little significance, because the 15% crite-

rion limits the acceptable values to only two for each element and, moreover, the uncertainties of these are either missed or no details on their estimate are given.

CONCLUSIONS

The experiment shows that for elements with photoabsorption threshold in the region of the incident-photon energy, i.e., 59.54 keV in the present case, the calculated values of the atomic coherent differential cross section exhibit regular observable deviations from the experimental ones, even when the accurate SMK procedure is employed. These deviations are probably caused by small differences in the values of some of the parameters employed in the calculations, the effects of which are amplified by the high gradient of such a cross section near the photoeffect threshold. In the present experiment the greatest regular deviations do not exceed 4–5 %. Moreover, the mean of all the SMK_N values differs from the unity of an amount much smaller than the relative uncertainty of the experimental data.

The MFK_N and RFC_N values as functions of both atomic number and angle show greater individual deviations, which can reach and exceed 10%, though only in very few cases. The mean of all the normalized values differs from the unity of a little more than $+7\%$ and -4% for MFK_N and RFC_N results, respectively, i.e., of an amount appreciably greater than that acceptable on the grounds of experimental uncertainties. However, such procedures make it possible to present the parameters needed for the calculations of the coherent-scattering amplitudes in a very simple tabular form as functions of the momentum transfer alone, i.e., of the quantity $\sin(\vartheta/2)/\lambda$, with ϑ scattering angle and λ wavelength of the incident radiation. In many applications, which do not require very rigorous individual values, the convenience of the use of these procedures, in data processing too, justifies their diffusion, and makes refinements and revisions always useful.

ACKNOWLEDGMENTS

The authors wish to thank Dr. L. Kissel for his kindness in performing SMK and MFK relevant calculations and Dr. J. H. Hubbell, who supplied useful tabulations of atomic data. Special thanks to Dr. E. Luppi for her help in facilitating the computer work, and to A. Magnani for his technical support. The authors are also grateful to MURST (Rome) and Regione Emilia-Romagna (Bologna) for their financial aid. One of us (B.S.) is especially obliged to ICTP (Trieste) for the grant that permitted him to participate in this experiment.

[1] R. H. Pratt, in *X-Ray and Inner Shell Processes*, edited by T. A. Carlson, M. O. Krause, and S. T. Manson (AIP, New York, 1990).
[2] G. Basavaraju, P. P. Kane, L. Kissel, and R. H. Pratt, Phys. Rev. A **49**, 3664 (1994).
[3] L. Kissel, B. Zhou, S. C. Roy, S. K. Sen Gupta, and R. H. Pratt, Acta Crystallogr. Sect. A **51**, 271 (1995).
[4] L. Kissel, R. H. Pratt, and S. C. Roy, Phys. Rev. A **22**, 1970 (1980).
[5] L. Kissel and R. H. Pratt, in *Atomic Inner-Shell Physics*, edited by B. Crasemann (Plenum, New York, 1985).
[6] J. H. Hubbell, W. J. Veigele, E. A. Briggs, R. T. Brown, D. T. Cromer, and R. J. Howerton, J. Phys. Chem. Ref. Data **4**, 471 (1975); **6**, 615(E) (1977).
[7] J. H. Hubbell and I. Øverbø, J. Phys. Chem. Ref. Data **8**, 69 (1979).
[8] W. Franz, Z. Phys. **95**, 652 (1935); **98**, 314 (1936).
[9] D. Y. Smith, Phys. Rev. A **35**, 3381 (1987).
[10] L. Kissel and R. H. Pratt, Acta Crystallogr. Sect. A **46**, 170 (1990).
[11] D. Schaupp, M. Schumacher, F. Smend, P. Rullhusen, and J. H. Hubbell, J. Phys. Chem. Ref. Data **12**, 467 (1983).
[12] R. Kronig, J. Opt. Soc. Am. **12**, 547 (1926).
[13] H. Kramers, Atti Congr. Fis. Como (1927) **2**, 545 (1927).
[14] D. T. Cromer and D. A. Liberman, J. Chem. Phys. **53**, 1891 (1970).
[15] D. T. Cromer, Acta Crystallogr. Sect. A **32**, 339 (1976).
[16] D. T. Cromer and D. A. Liberman, Acta Crystallogr. Sect. A **37**, 267 (1981).
[17] D. T. Cromer, in *International Tables for Crystallography*, edited by A. Ibers and W. C. Hamilton (Kynoch, Birmingham, 1974), Vol. IV.
[18] D. T. Cromer, J. Appl. Crystallogr. **16**, 437 (1983).
[19] B. L. Henke, P. Lee, T. J. Tanaka, R. L. Shimabukuro, and B. K. Fujikawa, At. Data Nucl. Data Tables **27**, 1 (1982).
[20] B. L. Henke, E. M. Gullikson, and J. C. Davis, At. Data Nucl. Data Tables **54**, 181 (1993).
[21] C. T. Chantler, J. Phys. Chem. Ref. Data **24**, 71 (1995).
[22] P. P. Kane, L. Kissel, R. H. Pratt, and S. C. Roy, Phys. Rep. **140**, 75 (1986).
[23] P. P. Kane, G. Basavaraju, S. M. Lad, K. M. Varier, L. Kissel, and R. H. Pratt, Phys. Rev. A **36**, 5626 (1987).
[24] S. S. Nandi, R. Dutta, and N. Chaudhuri, J. Phys. B **20**, 4027 (1987).
[25] F. Smend, D. Schaupp, H. Czerwinski, M. Schumacher, A. H. Millhouse, and L. Kissel, Phys. Rev. A **36**, 5189 (1987).
[26] C. Bui and M. Milazzo, Nuovo Cimento D **11**, 655 (1989).
[27] S. S. Nandi, S. K. Ghose, S. K. Sengupta, and N. Chaudhuri, J. Phys. B **22**, 1175 (1989).
[28] K. Siddappa, N. Govinda Nayak, K. M. Balakrishna, and N. Lingappa Shivaramu, Phys. Rev. A **39**, 5106 (1989).
[29] K. M. Varier and M. P. Unnikrishnan, Nucl. Instrum. Methods Phys. Res. A **280**, 428 (1989).
[30] N. Govinda Nayak, K. Siddappa, K. M. Balakrishna, and N. Lingappa, Phys. Rev. A **45**, 4490 (1992).
[31] G. Basavaraju, P. P. Kane, S. M. Lad, L. Kissel, and R. H. Pratt, Phys. Rev. A **51**, 2608 (1995).
[32] S. Erzeneoğlu, Y. Kurucu, R. Durak, and Y. Sahin, Phys. Rev. A **51**, 4628 (1995).
[33] L. Kissel (private communication).
[34] L. Kissel (private communication).
[35] E. Casnati, C. Baraldi, and A. Tartari, Phys. Rev. A **42**, 2627 (1990).

[36] E. Casnati, C. Baraldi, and A. Tartari, Phys. Rev. A **44**, 1699 (1991).
[37] C. M. Lederer and V. S. Shirley, *Table of Isotopes*, 7th ed. (Wiley, New York, 1978).
[38] E. Casnati, C. Baraldi, A. Tartari, and B. Singh, Appl. Radiat. Isot. **44**, 1155 (1993).
[39] W. J. Veigele, At. Data **5**, 51 (1973).
[40] E. Storm and H. I. Israel, Nucl. Data Tables A **7**, 565 (1970).
[41] E. F. Plechaty, D. E. Cullen, and R. J. Howerton, Lawrence Livermore Laboratory, Report No. UCRL 50400, 1981 (unpublished).
[42] J. H. Scofield, Lawrence Livermore Laboratory, Report No. UCRL 51326, 1973 (unpublished).
[43] F. Biggs, L. B. Mendelsohn, and J. B. Mann, At. Data Nucl. Data Tables **16**, 201 (1975).
[44] E. Casnati, A. Tartari, C. Baraldi, and G. Napoli, J. Phys. B **18**, 2843 (1985).
[45] D. Schaupp, H. Czerwinski, F. Smend, R. Wenskus, M. Schumacher, A. H. Millhouse, and H. Schenk-Strauss, Z. Phys. A **319**, 1 (1984).
[46] M. Schumacher and A. Stoffregen, Z. Phys. A **283**, 15 (1977).